

AN INNOVATIVE ELASTIC WHEEL - RAIL CONTACT MODEL

Silvia Magheri¹, Enrico Meli¹, Susanna Papini¹, Mirko Rinchi¹

¹*Department of Energy Engineering S. Stecco, University of Florence, Italy*
*Email: silvia.magheri@unifi.it, meli@mapp1.de.unifi.it,
susanna@mapp1.de.unifi.it, rinchi@mapp1.de.unifi.it*

Keywords: Multibody modeling, wheel-rail contact model, continuum mechanics.

SUMMARY. In this work the authors intend to present an innovative elastic wheel – rail contact model. The model considers the wheel and the rail as elastic deformable bodies and requires the numerical solution of the Navier’s elasticity equation. The contact between wheel and rail has been described by means of suitable analytical contact conditions. Subsequently the contact model has been inserted within the multibody model of a benchmark railway vehicle (the Manchester Wagon) in order to obtain a complete model of the wagon. The whole model has been implemented in the Matlab/Simulink environment and numerical simulations of the vehicle dynamics have been carried out on many different railway tracks with the aim of evaluating the performance of the model. In conclusion the main purpose of the authors is to achieve a better integration between the differential modeling and the multibody modeling, almost absent in literature (especially in the railway field).

1 INTRODUCTION

The multibody simulation of the railway vehicle dynamics needs a reliable contact model that satisfies the following specifics: accurate description of the global and local contact phenomena (contact forces, position and shape of the contact patch, stress and strain), general and robust handling of the multiple contact, high numerical efficiency and compatibility with commercial multibody software (Simpack Rail, Adams Rail).

The wheel – rail contact problem has been discussed by several authors and many models can be found in the literature. All the contact model specifically designed for the multibody modeling (as the so-called rigid contact formulation [1]-[3] and the semi-elastic contact description [2]-[4]) are computationally very efficient but their generality and accuracy turn out to be often insufficient. In particular, the physical theories behind this kind of models (Hertz's and Kalker's theory) require very restrictive hypotheses that, in many circumstances, are unverified.

Differential contact models are needed if a detailed description of the contact phenomena is required. In other words wheel and rail have to be considered elastic bodies governed by the Navier’s equations and the contact has to be described by suitable analytical contact conditions. This kind of approach assures high generality and accuracy but still needs very large computational costs and memory consumption [2] [5]-[8]. For this reason, the integration between multibody and differential modeling is almost absent in literature especially in the railway field. However this integration is very important because only the differential modeling allows an accurate analysis of the contact problem while the multibody modeling is the standard in the study of the railway dynamics.

In this work the authors intend to present an innovative differential contact model with the aim of achieving a better integration between multibody and differential modeling. The new contact model is fully 3D and satisfies all the specifics described above. The developed procedure requires

the discretization of the elastic contact problem (Navier's equations and analytical contact condition) and subsequently the solution of the nonlinear discrete problem. Both the steps have been implemented in Matlab/Simulink environment. At this point the contact model has been inserted within a 2D multibody model of a railway vehicle (Manchester Wagon [9]) to obtain a complete model of the wagon. The choice of a 2D multibody model allows to study the lateral vehicle dynamics and at the same time to reduce the computational load. The multibody model has been implemented in SimMechanics, a Matlab toolbox specifically designed for multibody dynamics. The 2D multibody model of the same vehicle (this time equipped with a standard contact model based on the semi – elastic approach) has been then implemented also in Simpack Rail, a commercial multibody software for railway vehicles widely tested and validated.

Finally numerical simulations of the vehicle dynamics have been carried out on many different railway tracks with the aim of evaluating the performance of the whole model. The comparison between the results obtained by the Matlab model and those obtained by the Simpack Rail model has allowed an accurate and reliable validation of the new contact model.

2 ARCHITECTURE OF THE MODEL

As said in the introduction the whole model consists of two different part: the 2D multibody model of the railway vehicle and the fully 3D differential wheel – rail contact model. The 2D model has been obtained from a fully 3D multibody model of the Manchester Wagon (see Fig.(1) and Chapter 4).

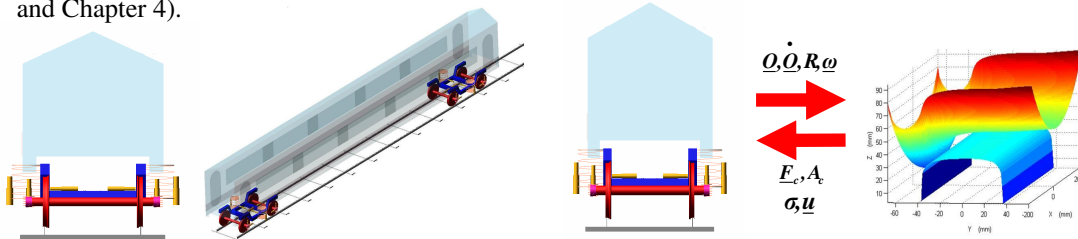


Fig.1: 2D/3D multibody models of the Manchester Wagon. Fig.2: General architecture of the model.

During the simulation the 2D multibody model interacts with the fully 3D differential contact model. The general architecture of the model is schematically shown in Fig. (2).

At each integration step the multibody model evaluates the kinematic variables relative to the wheelset and consequently to each wheel – rail pair. Starting from these quantities, the contact model calculates the global and local contact variables (force, contact patch, stress and displacement). Finally the knowledge of the contact variables allows the multibody model to carry on the simulation of the vehicle dynamics.

3 REFERENCE SYSTEMS

The railway track can be considered as a 3D curve $\underline{\gamma}(s)$ expressed in a fixed reference system $O_f x_f y_f z_f$ (where s is the curvilinear abscissa of $\underline{\gamma}$). Usually in the cartographic description of the track only the curvature $K(s)$ of $\underline{\gamma}(s)$ and the track slope $p(s)$ are known; however the knowledge of these parameters is enough to rebuild the curve $\underline{\gamma}(s)$. [10]

In this work the lateral vehicle dynamics will be described in a local reference system $O_R x_R y_R z_R$ having the x_R axis tangent to the track in the point $O_R = \underline{\gamma}(s)$ and the z_R axis normal to the plane of the rails. In the considered case the time histories of the curvilinear abscissa $s(t)$ and of the origin $O_R = \underline{\gamma}(s(t))$ are supposed to be known (for instance they can be calculated by

simulating independently the longitudinal vehicle dynamics). The local system follows the motion of the whole model along the track so that the centers of mass of the bodies lie always on the plane $y_R z_R$. According to chapter 2, the car – body and the bogie can only translate along y_R and z_R and rotate around x_R while the wheelset can also rotate around its symmetry axis.

Subsequently a third reference system $O_W x_W y_W z_W$ is defined. The origin O_W coincides with the center of mass of the wheelset and the y_W axis with its symmetry axis. This system is fixed to the wheelset except for the rotation around the y_W axis. The placement of the reference systems is illustrated in Fig. (3). In order to correctly describe the differential contact model, two further reference systems have to be defined for each wheel – rail pair. For the sake of simplicity only the left pair has been reported in Fig. (4).

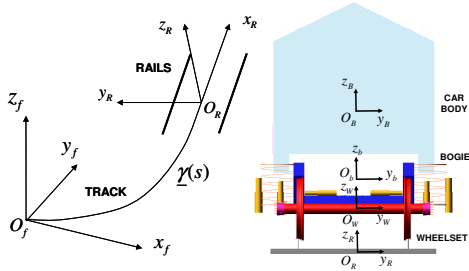


Fig.3: Reference systems relative to the multibody model.

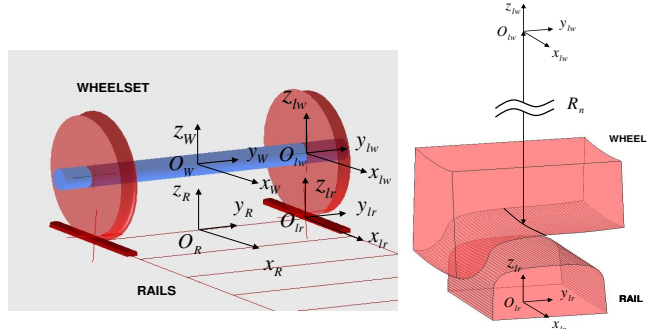


Fig.4: Reference systems relative to the differential contact model.

The first system $O_{lw} x_{lw} y_{lw} z_{lw}$ is parallel to the system $O_W x_W y_W z_W$ and its origin O_{lw} lies on the symmetry axis of the wheel. The system is fixed to the wheel except for the rotation around the y_{lw} axis. Moreover the origin O_{lw} belongs to the nominal rolling plane, i.e. the plane normal to the rotation axis containing the nominal rolling radius. The second system $O_{lr} x_{lr} y_{lr} z_{lr}$ is parallel to the system $O_R x_R y_R z_R$. Its origin O_{lr} belongs to the axis y_R while the distance between O_R and O_{lr} has to assure the correct gauge between the rails. Both the reference systems described above are very important because the global and local contact variables will be evaluated by the contact model just in these systems.

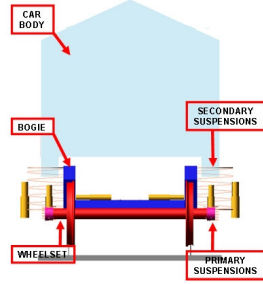
Finally, as regards the external forces acting on the bodies, some considerations are needed. As said before, the lateral vehicle dynamics is studied in the local reference system $O_R x_R y_R z_R$ but this system is not inertial. Therefore the multibody model will have to consider the effect of the fictitious forces (centrifugal force and Coriolis force). These quantities can be calculated starting from the knowledge of the kinematics of the bodies as a function of the curvature $K(s)$ and of the track slope $p(s)$. [10]

4 THE 2D MULTIBODY MODEL

The 2D multibody model has been obtained from a fully 3D multibody model of the Manchester Wagon, the physical and geometrical characteristics of which are easily available in the literature. [9] The original 3D model consists of: 1 car – body, 2 bogies and 4 wheelsets; rear and front primary suspensions; rear and front secondary suspensions (including roll bar, traction rod and bumpstop).

Both the primary and the secondary suspensions are usually modeled by means of nonlinear force elements like three- dimensional springs and dampers. The 2D model can be thought of as a section of the 3D model and comprises (Fig. (5)): one car – body, one bogie and one wheelset; one

primary suspension; one secondary suspension (including roll bar and bumpstop).



Body	Mass	Inertia
Car – body	0.25	0.25
Bogie	0.5	0.5
Wheelset	1	1

Table 1: Scaling factors (mass and inertia).

Suspensions	Springs	Dampers
Secondary	0.5	0.5
Primary	1	1

Table 2: Scaling factors (springs and dampers).

Fig.5: Reference systems relative to the differential contact model.

As regards the bodies, only some DOF are allowed by the 2D model: the car – body and the bogie have 3 DOF (they can translate along the axes y_R and rotate around the x_R axis); the wheelset, considered as a 3D body, has 4 DOF (besides the previous DOF it can also rotate around its symmetry axis y_W). Moreover, in order to assure the dynamic equivalence between the 2D model and the original 3D model, the inertial characteristics of the bodies and the physical characteristics of the force elements have to be correctly scaled down.[3][9] The values of the scaling factors are schematically reported in Tab. (1) and Tab. (2).

The choice of a 2D multibody model has been made with the aim of studying the lateral vehicle dynamics and, at the same time, of reducing the computational load. In the near future fully 3D multibody models of the Manchester Wagon will be considered in order to have a complete description of the vehicle dynamics.

5 THE 3D DIFFERENTIAL CONTACT MODEL

As regards the generic contact variable Z , the following convention will be adopted:

- Z_w and Z_w^r will denote a variable relative to the wheel respectively expressed in the reference systems $O_{l_w}x_{l_w}y_{l_w}z_{l_w}$ and $O_{l_r}x_{l_r}y_{l_r}z_{l_r}$
- Z_r and Z_r^w will denote a variable relative to the rail respectively expressed in the reference systems $O_{l_r}x_{l_r}y_{l_r}z_{l_r}$ and $O_{l_w}x_{l_w}y_{l_w}z_{l_w}$.

In the future, according to this convention, the various changes of reference system won't be continually remarked but will be taken for granted.

5.1 Inputs and Outputs

The contact model can be thought of as a black box having the following inputs and outputs:

- INPUTS: the kinematic variables relative to the considered wheel – rail pair (in this case the left one), i.e. the position \underline{O}_w^r , the velocity \underline{O}_w^r , the orientation R_w^r and the angular velocity $\underline{\omega}_w^r$ of the reference system $O_{l_w}x_{l_w}y_{l_w}z_{l_w}$ with respect to the system $O_{l_r}x_{l_r}y_{l_r}z_{l_r}$ (Fig. (4)).
- OUTPUTS: the global and local contact variables relative to the wheel and to the rail, like the contact forces \underline{F}_{wC} and \underline{F}_{rC} , the stresses σ_w and σ_r , the displacements \underline{u}_w and \underline{u}_r and the contact patches A_{wC} and A_{rC} .

5.2 The kinematics of the problem

The wheel and the rail have been considered as two linear elastic bodies Ω_w and Ω_r (as shown in Fig. (6)). [6][7] Both the domains are supposed to be sufficiently large compared to the dimensions of the contact patch. The boundaries $\partial\Omega_w$ and $\partial\Omega_r$ are split into two disjoint regions,

respectively Γ_{wD} , Γ_{wC} and Γ_{rD} , Γ_{rC} . Within the regions Γ_{wD} and Γ_{rD} the displacements are fixed (and equal to zero) while Γ_{wC} and Γ_{rC} (dashed in the figure) are the regions where the contact may occur. In case of contact the geometric intersection between the surfaces Γ_{wC} and Γ_{rC} (and thus between the non-deformed configurations) allows to define two regions $\tilde{A}_{wC} \subset \Gamma_{wC}$ and $\tilde{A}_{rC} \subset \Gamma_{rC}$ (with $\tilde{A}_{wC} \simeq \tilde{A}_{rC}$) that can be considered as a rough estimate of the contact areas. The situation is schematically sketched in Fig. (6) and Fig. (7).

The real contact areas $A_{wC} \subset \tilde{A}_{wC}$ and $A_{rC} \subset \tilde{A}_{rC}$ (with $A_{wC} \simeq A_{rC}$) are unknown and have to be calculated by the model. For this purpose a contact map $\underline{\Phi}$ has to be introduced. The contact map $\underline{\Phi}: \tilde{A}_{wC} \rightarrow \tilde{A}_{rC}$ (by convention the wheel is the master body) locates the position of the point $\underline{\Phi}(\underline{x}_w^r) \in \tilde{A}_{rC}$ that will come in contact with the generic point $\underline{x}_w^r \in \tilde{A}_{wC}$. In this case the map $\underline{\Phi}$ is defined as the normal projection $\underline{\Phi}(\underline{x}_w^r)$ of the point $\underline{x}_w^r \in \tilde{A}_{wC}$ on the surface \tilde{A}_{rC}

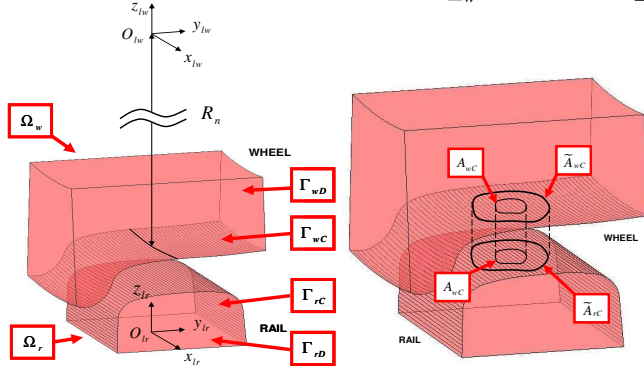


Fig. 6: The problem geometry

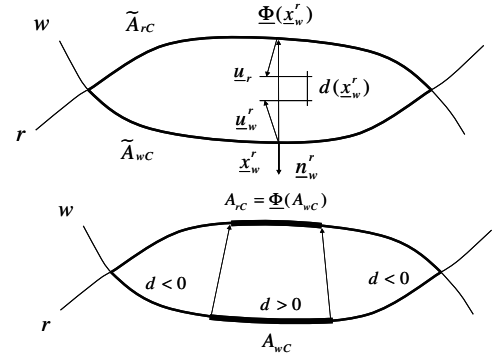


Fig.7: Contact map and distance function.

Starting from the contact map, the distance function between the deformed configurations $d: \tilde{A}_{wC} \rightarrow R$ can be evaluated:

$$d(\underline{x}_w^r) = (\underline{u}_w^r - \underline{u}_r) \cdot \underline{n}_w^r - (\underline{\Phi}(\underline{x}_w^r) - \underline{x}_w^r) \cdot \underline{n}_w^r \quad (1)$$

where \underline{n}_w^r is the outgoing normal versor to the surfaces Γ_{wC} . The function d is positive if there is penetration between the deformed configurations and negative otherwise.

Formally the contact area A_{wC} is defined as the region of \tilde{A}_{wC} where the function d is positive while the contact area $A_{rC} = \underline{\Phi}(A_{wC})$ is the normal projection of A_{wC} on \tilde{A}_{rC} . In other words, from a kinematic point of view, the penetration between the deformed bodies is allowed and will play a fundamental role in the contact model (see paragraph 5.3). [6][7]

In this way the estimated contact areas \tilde{A}_{wC} and \tilde{A}_{rC} depend only on the relative wheel – rail kinematics ($\underline{Q}_w^r, \underline{Q}_r^r, \underline{R}_w^r$ and $\underline{\omega}_w^r$) while the real contact areas A_{wC} and A_{rC} depend also on the displacements \underline{u}_w and \underline{u}_r . Finally it is useful to remark that no hypothesis has been made on the shape of the contact patch; in particular, the contact patch can be formed of one or more disjoint parts. As regards the wheel and rail profiles, the standard ORES1002 and UIC60 have been used.[10]

5.3 The contact model

According to the linear theory of elasticity [6] [7], both the wheel and the rail are governed by the Navier's equations:

$$\begin{aligned} \text{div } \underline{\sigma}_w(\underline{u}_w) &= \underline{0} \quad \text{on } \Omega_w, \quad \underline{\sigma}_w(\underline{u}_w) \underline{n}_w = \underline{p}_w \quad \text{on } \tilde{A}_{wC}, \quad \underline{u}_w = \underline{0} \quad \text{on } \Gamma_{wD}, \quad \underline{\sigma}_r(\underline{u}_r) \underline{n}_r = \underline{p}_r \quad \text{on } \tilde{A}_{rC} \quad (2) \\ \text{div } \underline{\sigma}_r(\underline{u}_r) &= \underline{0} \quad \text{on } \Omega_r, \quad \underline{\sigma}_w(\underline{u}_w) \underline{n}_w = \underline{0} \quad \text{on } \Gamma_{wC} \setminus \tilde{A}_{wC}, \quad \underline{u}_r = \underline{0} \quad \text{on } \Gamma_{rD}, \quad \underline{\sigma}_r(\underline{u}_r) \underline{n}_r = \underline{0} \quad \text{on } \Gamma_{rC} \setminus \tilde{A}_{rC} \\ &\text{where } \underline{n}_w \text{ and } \underline{n}_r \text{ are the outgoing normal vectors to the surfaces } \Gamma_{wC} \text{ and } \Gamma_{rC} \text{ while } \underline{p}_w \text{ and } \end{aligned}$$

\underline{p}_r are the unknown contact pressures. The pressures \underline{p}_w and \underline{p}_r are defined on \tilde{A}_{wC} and \tilde{A}_{rC} but, according to paragraph 5.2, will have to be zero on $\tilde{A}_{wC} \setminus A_{wC}$ and $\tilde{A}_{rC} \setminus A_{rC}$. Both the bodies have the material characteristics of the steel (Young's modulus $E_w = E_r = 2.1 \cdot 10^{11} Pa$ and Poisson's coefficient $\nu_w = \nu_r = 0.3$). In the studied case the volume forces (i. e. the gravity) have been neglected because the multibody model of the wheelset already considers their effect. Moreover, since the solution is supposed to be steady within the integration step (see Fig. (2)), also the inertial terms have been omitted.

Equivalently the problem (2) can be formulated in weak form as follows:

$$\int_{\Omega_w} \underline{\sigma}_w(\underline{u}_w) : \underline{\varepsilon}_w(\underline{v}_w) dV = \int_{\tilde{A}_{wC}} \underline{p}_w \cdot \underline{v}_w dA \quad \forall \underline{v}_w \in V_w, \quad \int_{\Omega_r} \underline{\sigma}_r(\underline{u}_r) : \underline{\varepsilon}_r(\underline{v}_r) dV = \int_{\tilde{A}_{rC}} \underline{p}_r \cdot \underline{v}_r dA \quad \forall \underline{v}_r \in V \quad (3)$$

where $\underline{\varepsilon}_w$ and $\underline{\varepsilon}_r$ are the strains while V_w and V_r are suitable Sobolev's spaces.

In order to complete the contact model, the contact pressures \underline{p}_w and \underline{p}_r have to be expressed as a function of the displacements \underline{u}_w and \underline{u}_r . For the sake of simplicity the normal and the tangential contact pressures on the wheel are introduced: $p_{wN}^r = \underline{p}_w \cdot \underline{n}_w^r$, $\underline{p}_{wT}^r = \underline{p}_w - p_{wN}^r \underline{n}_w^r$. The normal pressure p_{wN}^r has been calculated by means of the distance function d :

$$p_{wN}^r(\underline{x}_w^r) = -K \max(d(\underline{x}_w^r), 0) \quad \text{on } \tilde{A}_{wC} \quad (4)$$

where $K > 0$ is a fictitious stiffness constant. The value of K have to be chosen large enough to assure the accuracy required by this kind of problems. The condition of ideal contact (total absence of penetration between the deformed bodies) is reached for $K \rightarrow +\infty$ (usually $K \geq 10^4 \text{ N/m}^3$). [6][7] To evaluate the tangential pressure \underline{p}_{wT}^r , the slip \underline{s}_{wT}^r between the wheel and rail surfaces has to be defined. Since the solution is supposed to be steady within the integration step, the following expression holds: [2]

$$\underline{s}_{wT}^r(\underline{x}_w^r) = \underline{w}_w^r(\underline{x}_w^r) + \underline{u}_r^r(\underline{x}_w^r) - \underline{w}_r^r(\underline{\Phi}(\underline{x}_w^r)) - \underline{u}_w^r(\underline{\Phi}(\underline{x}_w^r)) = \underline{w}_w^r(\underline{x}_w^r) + J_w^r(\underline{x}_w^r) \underline{w}_w^r(\underline{x}_w^r) - \underline{w}_r^r(\underline{\Phi}(\underline{x}_w^r)) - J_r^r(\underline{\Phi}(\underline{x}_w^r)) \underline{w}_r^r(\underline{\Phi}(\underline{x}_w^r)) \quad (5)$$

where \underline{w}_w^r and \underline{w}_r^r are the rigid velocity of the points \underline{x}_w^r and $\underline{\Phi}(\underline{x}_w^r)$ while J_w^r and J_r^r are the Jacobians of \underline{u}_w^r and \underline{u}_r^r . As usual the normal and the tangential slips are: $s_{wN}^r = \underline{s}_{wT}^r \cdot \underline{n}_w^r$, $\underline{s}_{wT}^r = \underline{s}_{wT}^r - s_{wN}^r \underline{n}_w^r$. According to the standard friction models, the tangential pressures $\underline{p}_{wT}^r = \underline{p}_{wT}^r(\underline{x}_w^r)$ can be expressed as follows:

$$\underline{p}_{wT}^r = -\mu(s_{wT}^r, V) |p_{wN}^r| \frac{\underline{s}_{wT}^r}{s_{wT}^r} \quad \text{on } \tilde{A}_{wC} \quad (6)$$

where s_{wT}^r is the norm of $\underline{s}_{wT}^r = \underline{s}_{wT}^r(\underline{x}_w^r)$ and V is the longitudinal velocity of the vehicle. Further details on the friction function $\mu(s_{wT}^r, V)$ can be found in the literature. [10]

Finally the action - reaction principle (the Newton's Third Law) allows to calculate the pressures \underline{p}_r : $\underline{p}_r(\underline{\Phi}(\underline{x}_w^r)) = -\underline{p}_{wT}^r(\underline{x}_w^r)$ on \tilde{A}_{wC} . It is useful to remark that, according to the described model, the pressures \underline{p}_w and \underline{p}_r are zero respectively on $\tilde{A}_{wC} \setminus A_{wC}$ and $\tilde{A}_{rC} \setminus A_{rC}$.

The displacements \underline{u}_w and \underline{u}_r will be evaluated in the following through the numerical solution of Eq. (3). The knowledge of these unknown quantities will allow to calculate all the other required outputs like the contact areas A_{wC} and A_{rC} and the stresses $\underline{\sigma}_w$ and $\underline{\sigma}_r$. The contact forces \underline{F}_{wC} and \underline{F}_{rC} will be estimated by integration: $\underline{F}_{wC} = \int_{\tilde{A}_{wC}} \underline{p}_w dA$, $\underline{F}_{rC} = \int_{\tilde{A}_{rC}} \underline{p}_r dA$.

5.4 The discretization of the model

Both the elastic bodies have been discretized by means of tetrahedral elements and linear shape functions. The meshes have been built according to the standard Delaunay's algorithms (Fig. (8)). [8] The resolution of the meshes on the surfaces Γ_{wC} and Γ_{rC} is constant (usually in the range $1\text{mm} \div 2\text{mm}$) because the position and the dimensions of the contact patch are a priori unknown.

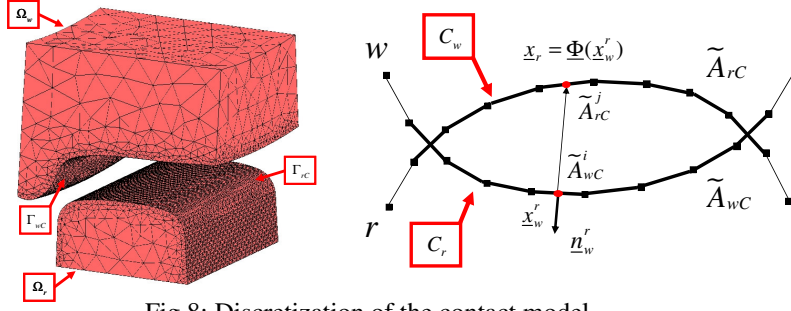


Fig.8: Discretization of the contact model.

The surface resolution has also to assure an accuracy enough to correctly describe the contact phenomena. Moreover it is important to remark that the meshes have been created directly in the reference systems $O_{lw}x_{lw}y_{lw}z_{lw}$ and $O_{lr}x_{lr}y_{lr}z_{lr}$; therefore they don't change during the simulation and can be easily built off – line.

In the future the following convention will be adopted. The sets of all the elements of wheel and rail will be called T_w and T_r while the vectors $\underline{u}_{wh}, \underline{u}_{rl} \in R^{12}$ will contain the displacements of the four nodes belonging to the elements $h \in T_w$ and $l \in T_r$. Finally the vectors \underline{U}_w and \underline{U}_r will comprise the displacements relative to all the nodes of wheel and rail. Since the displacements on Γ_{wD} and Γ_{rD} are zero, the dimension of \underline{U}_w , \underline{U}_r are $3(N_w - N_{wD})$ and $3(N_r - N_{rD})$, where N_w and N_r are the numbers of nodes of wheel and rail while N_{wD} and N_{rD} are the numbers of nodes on Γ_{wD} and Γ_{rD} . Similarly C_w and C_r will be the sets of the active contact elements on wheel and on rail, i. e. the sets of the elements having respectively a face \tilde{A}_{wC} and \tilde{A}_{rC} that lies on \tilde{A}_{wC} and \tilde{A}_{rC} . The vectors $\underline{u}_{wi}, \underline{u}_{rj} \in R^{12}$ will contain the displacements of the four nodes belonging to the elements $i \in C_w$ and $j \in C_r$ while the vectors \underline{U}_{wC} and \underline{U}_{rC} will comprise the displacements relative to all the active elements. The dimension of \underline{U}_{wC} , \underline{U}_{rC} are $3N_{wC}$ and $3N_{rC}$ where N_{wC} and N_{rC} are the number of nodes belonging to the active elements. The knowledge of the relative kinematics (\underline{Q}_w^r , \underline{Q}_w^r , R_w^r and $\underline{\omega}_w^r$) and consequently of the estimated contact areas \tilde{A}_{wC} and \tilde{A}_{rC} allows to determine the sets C_w and C_r of the active contact elements on the wheel and on the rail.

For each active contact element on the wheel, the center \underline{x}_{wi}^r of the face \tilde{A}_{wC}^i is considered. The normal projection $\underline{x}_{rj}^r = \Phi(\underline{x}_{wi}^r)$ of \underline{x}_{wi}^r on \tilde{A}_{rC} will belong to the external face \tilde{A}_{rC}^j of the j -th active contact element on the rail. In particular the index $j(i)$ will be a function of the index i . In other words the pairs of points (\underline{x}_{wi}^r , $\underline{x}_{rj(i)}^r$) with $i \in C_w$ can be thought of as the discretization of the contact map Φ . The situation is schematically sketched in Fig. (8).

The values of the displacements \underline{u}_{wi}^r , \underline{u}_{rj}^r and of their Jacobians J_w^r , J_r^r in the points \underline{x}_{wi}^r and \underline{x}_{rj}^r are evaluated through the shape functions. [6] [7] [8]

At this point the distance function $d_i = d(\underline{x}_{wi}^r)$ and the pressure $\underline{p}_{wi}^r = \underline{p}_{wi}^r(\underline{x}_{wi}^r)$ on the face \tilde{A}_{wC}^i of the active element of the wheel can be calculated by means of Eq. (1), (4) and (6). Finally a discrete version of the action – reaction principle (the Newton's Third Law) is needed to evaluate the pressure $\underline{p}_{rj}^r = \underline{p}_{rj}^r(\underline{x}_{rj}^r)$ on the face \tilde{A}_{rC}^j of the active element of the rail: $|\tilde{A}_{rC}^j| \underline{p}_{rj}^r = |\tilde{A}_{wC}^i| \underline{p}_{wi}^r$, where $|\tilde{A}_{wC}^i|$ and $|\tilde{A}_{rC}^j|$ are the areas of the faces \tilde{A}_{wC}^i and \tilde{A}_{rC}^j . Both the pressures \underline{p}_{wi}^r and \underline{p}_{rj}^r are supposed to be constant on \tilde{A}_{wC}^i and \tilde{A}_{rC}^j . The standard FEM techniques allow to discretize the weak form of the contact problem (see Eq. (3)) : [6] [7] [8]

$$\int_{\Omega_w} \sigma_w(\underline{u}_w) : \varepsilon(\underline{v}_w) dV = \sum_{h \in T_w} \underline{u}_{wh}^T K_{wh} \underline{v}_{wh} = \underline{U}_w^T K_w \underline{V}_w, \quad \int_{\Omega_r} \sigma_r(\underline{u}_r) : \varepsilon(\underline{v}_r) dV = \sum_{l \in T_r} \underline{u}_{rl}^T K_{rl} \underline{v}_{rl} = \underline{U}_r^T K_r \underline{V}_r \quad (7)$$

$$\int_{\tilde{A}_{wC}} \underline{p}_w \cdot \underline{v}_w dA = \sum_{i \in C_w} \underline{p}_{wi}^T M_{wi} \underline{v}_{wi} = \underline{F}_w(\underline{U}_{wC}, \underline{U}_{rC})^T \underline{V}_w, \quad \int_{\tilde{A}_{rC}} \underline{p}_r \cdot \underline{v}_r dA = \sum_{j \in C_r} \underline{p}_{rj}^T M_{rj} \underline{v}_{rj} = \underline{F}_r(\underline{U}_{wC}, \underline{U}_{rC})^T \underline{V}_r$$

where K_{wh} , K_{rl} are the stiffness matrices relative to the elements $h \in T_w$, $l \in T_r$ and M_{wi} , M_{rj} depend on the shape functions. The global stiffness matrices K_w and K_r are symmetric,

positive defined and sparse while the vectors \underline{F}_w and \underline{F}_r , that contain the terms due to the contact pressures, are sparse. The dimensions of the stiffness matrices are about $10000 \div 100000$ but they are evaluated directly in the reference systems $O_{lw}x_{lw}y_{lw}z_{lw}$ and $O_{lr}x_{lr}y_{lr}z_{lr}$; therefore they don't change during the simulation and can be easily built off – line. Eq. (3) and Eq. (7), combined together, give

$$\underline{U}_w^T K_w \underline{V}_w = \underline{F}_w(\underline{U}_{wC}, \underline{U}_{rC})^T \underline{V}_w \quad \forall \underline{V}_w \in R^{3(N_w - N_{wD})}, \quad \underline{U}_r^T K_r \underline{V}_r = \underline{F}_r(\underline{U}_{wC}, \underline{U}_{rC})^T \underline{V}_r \quad \forall \underline{V}_r \in R^{3(N_r - N_{rD})} \quad (8)$$

Finally, since the matrices K_w , K_r are symmetric and the vectors \underline{V}_w , \underline{V}_r are arbitrary, the following nonlinear system of algebraic equations is obtained:

$$K_w \underline{U}_w = \underline{F}_w(\underline{U}_{wC}, \underline{U}_{rC}), \quad K_r \underline{U}_r = \underline{F}_r(\underline{U}_{wC}, \underline{U}_{rC}) \quad (9)$$

where, as said before, the contact displacements \underline{U}_{wC} , \underline{U}_{rC} are a subset of the displacements \underline{U}_w , \underline{U}_r . Eq. (9) can be also written as

$$\underline{U}_w = H_w \underline{F}_w(\underline{U}_{wC}, \underline{U}_{rC}), \quad \underline{U}_r = H_r \underline{F}_r(\underline{U}_{wC}, \underline{U}_{rC}) \quad (10)$$

where the matrices $H_w = K_w^{-1}$ and $H_r = K_r^{-1}$ are symmetric, positive defined and full (consequently their storage can require a high memory consumption). Like K_w and K_r they don't change during the simulation and can be calculated off – line. Splitting \underline{U}_w , \underline{U}_r into contact displacement \underline{U}_{wC} , \underline{U}_{rC} and non – contact displacement \underline{U}_{wNC} , \underline{U}_{rNC} , Eq. (10) becomes

$$\begin{pmatrix} \underline{U}_{wNC} \\ \underline{U}_{wC} \end{pmatrix} = \begin{bmatrix} H_w^{11} & H_w^{12} \\ H_w^{21} & H_w^{22} \end{bmatrix} \begin{pmatrix} \underline{0} \\ \underline{f}_w(\underline{U}_{wC}, \underline{U}_{rC}) \end{pmatrix}, \quad \begin{pmatrix} \underline{U}_{rNC} \\ \underline{U}_{rC} \end{pmatrix} = \begin{bmatrix} H_r^{11} & H_r^{12} \\ H_r^{21} & H_r^{22} \end{bmatrix} \begin{pmatrix} \underline{0} \\ \underline{f}_r(\underline{U}_{wC}, \underline{U}_{rC}) \end{pmatrix} \quad (11)$$

In this way the second and the fourth components of Eq. (11) are sufficient to calculate contact displacement \underline{U}_{wC} , \underline{U}_{rC} :

$$\underline{U}_{wC} = H_w^{22} \underline{f}_w(\underline{U}_{wC}, \underline{U}_{rC}), \quad \underline{U}_{rC} = H_r^{22} \underline{f}_r(\underline{U}_{wC}, \underline{U}_{rC}) \quad (12)$$

The matrices H_w^{22} and H_r^{22} have the same properties of H_w and H_r but this time their dimensions are much smaller (about $100 \div 1000$). In particular, the dimension of H_w^{22} and H_r^{22} depend on the number of active elements that change during the simulation; therefore they have to be built directly on – line. The vectors \underline{f}_w and \underline{f}_r are full.

The remaining non – contact displacements \underline{U}_{wNC} , \underline{U}_{rNC} can be evaluated by means of the first and the third components of Eq. (11). The knowledge of the displacements \underline{U}_w , \underline{U}_r , evaluated by solving Eq. (9) or Eq. (12), allows to calculate all the other required outputs like the contact areas A_{wC} and A_{rC} and the stresses σ_w and σ_r . The contact forces \underline{F}_{wC} and \underline{F}_{rC} are estimated by numerical integration:

$$\underline{F}_{wC} = \sum_{i \in C_w} |\tilde{A}_{wC}^i| \underline{p}_{wi}, \quad \underline{F}_{rC} = \sum_{j \in C_r} |\tilde{A}_{rC}^j| \underline{p}_{rj}. \quad (13)$$

5.5 The SIMPACK RAIL 2D multibody model

The same multibody model of the benchmark vehicle (Manchester Wagon [9]) has been implemented also in Simpack Rail, a widely tested and validated multibody software for the analysis of the railway vehicle dynamics. This time the multibody model is equipped with a standard contact model based on the semi – elastic approach. [2]-[4] As in the previous case the 2D multibody model (designed for the study of the lateral dynamics) has been obtained from the fully 3D multibody model of the vehicle while the contact model is completely 3D (see Fig. (9)). The comparison between the results obtained by the Matlab/Simulink model and those obtained by the Simpack Rail model has allowed an accurate and reliable validation of the new contact model.

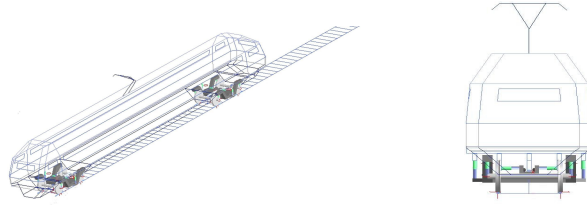


Fig.9: 3D and 2D multibody models of the Manchester Wagon (Simpack Rail).

5.6 Simulation of the lateral vehicle dynamics

The comparison between the Matlab/Simulink model (implemented on Matlab R2007b) and the Simpack Rail model (implemented on Simpack 8.900) has been carried out on the same curvilinear railway track, the data of which are reported in Tab. (3). [3] [10] The numerical data relative to the Matlab model and to the Simpack model are reported in Tab. (4) and Tab. (5).

Curvature	K	$1/1200 \text{ m}^{-1}$
Slope	P	0
Cant	β	60 mm
Laying angle	α_p	$1/40 \text{ rad}$
Velocity	V	45 m/s
Friction coefficient	μ	0.3

MATLAB model	
Differential Contact Model	Eq. (12)
ODE solver [11]	ODE 23
RelTol/AbsTol (ODE solver)	$10^{-8} / 10^{-6}$
Non-linear solver	Newton BICGStab

SIMPACK model	
Contact Model	Semi-Elastic Approach
ODE Solver [11]	ODE 5
Fixed Step	$5 * 10^{-4}$

Table 3: Data of the railway track

Table 4: Numerical Data

Table 5: Numerical Data

Among all the kinematic and dynamic variables evaluated by the models, the time histories of the following quantities are reported (for the sake of simplicity all the outputs are expressed in the reference system $O_R x_R y_R z_R$): the lateral displacement y_W^R of the centre of mass of the wheelset O_W^R (Fig. (10)) and the contact force on the left wheel \underline{F}_{lw}^R (in particular Y_{lw}^R is the lateral force (Fig. (11)) while Q_{lw}^R is the vertical forces (Fig. (12))).

The Matlab variables are plotted in blue while the equivalent Simpack quantities in red.

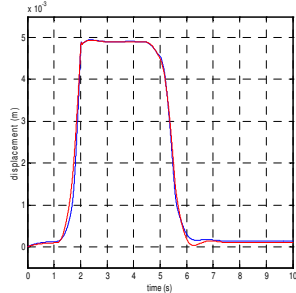


Fig. 10: Lateral displacement y_W^R

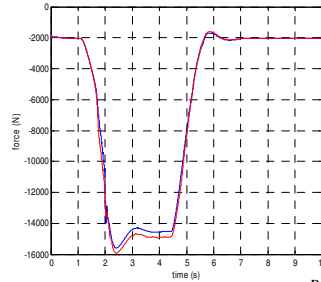


Fig. 11: Lateral force Y_{lw}^R

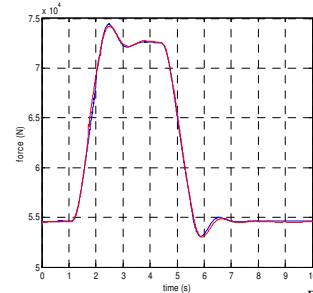


Fig. 12: Vertical force Q_{lw}^R

The simulation results show a good agreement between the Matlab model and the Simpack model both in terms of kinematic variables and in terms of contact forces.

As regards the positions of contact patches A_{wC} , A_{rC} on the wheel and on the rail, in order to give an effective description of the shifting of the contact areas during the simulation, a lateral section along the plane $y_R z_R$ of the areas A_{wC} , A_{rC} has been considered. The sections of the contact patches have been plotted on cylindrical surfaces generated by the wheel and rail profiles and as long as the distance traveled by the vehicle. By way of example the contact areas A_{wC} and A_{rC} on the left wheel and rail surfaces are reported in Fig. (13) and Fig. (14).

The sections of the contact areas evaluated by the Matlab model are plotted in blue while the contact points detected by the Simpack model are plotted in black. It is interesting to remark that, during the curve, a second contact point appears on the left wheel and rail (the track turns to left).

Consequently, while the Simpack model detects two distinct contact points, the contact areas evaluated by the Matlab model consist of two disjoint parts.

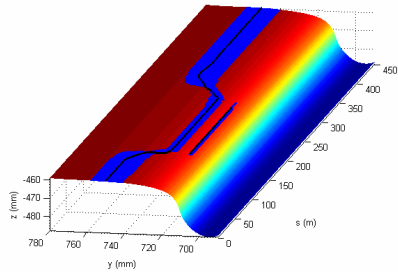


Fig.13: Section of contact area A_{lwC}

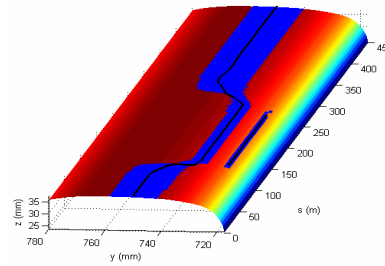


Fig.14: Section of contact area A_{lrC}

Also in this case the agreement between the results obtained by the Matlab model and the Simpack model is good.

In conclusion the accuracy of the Matlab model turns out to be comparable with that of the Simpack model; moreover the quasi – total absence of numerical noise highlights the robustness and the stability of the new differential contact model.

6 CONCLUSION AND PERSPECTIVE

The performances of the Matlab model turned out to be good both in terms of output accuracy and in terms of numerical efficiency and satisfy all the specifics reported in the introduction.

As regards the further developments, in the near future fully 3D multibody models of the Manchester Wagon will be considered. This kind of model allows a complete description of the vehicle dynamics but obviously involves an increase of the model DOFs and of the number of wheel – rail contact pairs. Moreover many optimizations of the differential contact model are planned for the future. The improvements will regard especially the FEM techniques used to discretize the contact problem. In particular new mesh generation algorithms and suitable nonlinear shape functions will be examined. These techniques assure a better accuracy in the description of the local contact phenomena but increases the dimension of the discrete problem and consequently the computational load and the memory consumption. Finally the implementation of the contact model in programming environments like C/C++ and FORTRAN will be considered in order to obtain a further reduction of the computation time.

References

- [1] Shabana, A.A. and Sany J.R., “An augmented formulation for mechanical systems with non-generalized coordinate”, *Nonlinear Dynamics*, **24**, 183-204 (2001).
- [2] Kalker, J.J., *Three – dimensional Elastic Bodies in Rolling Contact*, Kluwer Academic Publishers, Dordrecht, Netherlands (1990).
- [3] Dukkipati, R.V. and Amyot, J.R., *Computer Aided Simulation in Railway Dynamics*, Dekker, New York, 1988.
- [4] Shabana, A.A., Zaazaa, K.E., Escalona, J. L. and Sany, J. L., “Development of elastic force model for wheel/rail contact problems”, *Journal of Sound and Vibration*, **269**, 295-325 (2004).
- [5] Johnson, K.L., *Contact Mechanics*, Cambridge University Press, Cambridge, England, 1985
- [6] Kikuchi, N. and Oden, J.T., *Contact Problems in Elasticity*, SIAM Studies in Applied Mathematics, Philadelphia, Pennsylvania (1988).
- [7] Wriggers, P., *Computational Contact Mechanics*, Wiley&Sons, Hoboken, New Jersey, (2002).
- [8] Zienkiewicz, O., *The Finite Element Method in Engineering Science*, McGraw – Hill, New York (1988).
- [9] Iwinicki, S., *The Manchester Benchmarks for Rail Vehicle Simulators*, Swets & Zeitlinger, Lisse, Netherlands (1999).
- [10] Esveld, C., *Modern Railway Track*, Delft University of Technology, Delft, Netherlands, 2001.
- [11] Shampine, L.F. and Reichelt, M.W., “The MATLAB ODE Suite”, *SIAM Journal on Scientific Computing*, **18**, 1-22 (1997).